Phenotypic plasticity as an important mechanism of cave colonization and adaptation in *Astyanax* cavefish

Helena Bilandžija[1, 2], Breanna Hollifield[1], Mireille Steck[3], Guanliang Meng[4,5], Mandy Ng[1], Andrew D. Koch[6], Romana Gračan[7], Helena Ćetković[2], Megan L. Porter[3], Kenneth J. Renner[6], William R. Jeffery[1]

[1]Department of Biology, University of Maryland, College Park, MD 20742 USA
[2]Department of Molecular Biology, Ruđer Bošković Institute, Zagreb 10000, Croatia
[3]Department of Biology, University of Hawai'i at Mānoa, Honolulu, HI 96822 USA
[4]BGI-Shenzhen, Shenzhen 518083, China
[5]China National GeneBank, BGI-Shenzhen, Shenzhen 518120, China
[6]Department of Biology, University of South Dakota, Vermillion SD 57069 USA
[7]Department of Biology, Faculty of Science, University of Zagreb, 10000 Zagreb, Croatia

ABSTRACT

Subterranean habitats offer excellent opportunities to understand how adaptive phenotypes originate in changing environments. Cave dwelling animals show a suite of specialized traits associated with survival in a highly specialized dark environment. A widely accepted model for the evolution of cave animals posits cave colonization by surface dwelling ancestors followed by the acquisition of adaptive traits by standing genetic variation or new mutations over many generations. However, the speed of cave adaptation in some species is difficult to reconcile with this conventional viewpoint, suggesting the importance of alternative mechanisms operating over shorter timescales. To address these mechanisms, we exposed *Astyanax mexicanus* surface fish (SF) to completely dark (D/D) conditions during early development and compared them to siblings placed on a standard photoperiod (L/D). We identified multiple traits that were altered in D/D SF compared to L/D SF adults raised in complete darkness for up to 2 years. On a transcriptome level, these changes included differences in the expression of 356 genes related to sensory systems, endocrine signaling, circadian rhythms, the blood, and numerous metabolic changes, especially in lipids. On a phenotypic level, we found alterations in eye anatomy, pigmentation, metabolic rates, starvation resistance, hormone levels, and neurotransmitter levels. Remarkably, most of these alterations are associated with known adaptations to the cave environment that change in the direction of the cavefish phenotype. Contrary to the widely accepted view that cave-related traits result from long-term genetic processes, our results indicate that some traits can appear within a single generation by phenotypic plasticity. We also show that plasticity is a developmental and evolvable trait and that the initial plastic responses are random in terms of their adaptive outcome but may determine the subsequent course of adaptive evolution. Our study suggests that phenotypic plasticity may significantly contribute to the rapid evolution of cave-related traits providing a foundation for genetic assimilation in colonization of *A. mexicanus* to dark cave environments.

INTRODUCTION

A major problem in modern biology is understanding how organisms adapt to an environmental change and how complex, adaptive phenotypes originate. Phenotypic evolution can result from standing genetic variation, new mutations, or phenotypic plasticity followed by genetic assimilation, but these processes are often difficult to distinguish in slowly changing environments. This difficulty can be overcome by studying adaptation to more abrupt environmental changes, such as the dramatic transition from life on the Earth's surface to subterranean voids and caves.

A unifying feature of subterranean environments is complete darkness [1,2]. Cave-adapted animals have evolved a range of unusual and specialized traits, often called troglomorphic traits, which enable survival in challenging conditions of the subsurface. In cave dwelling animals, visual senses and protection from the effects of sunlight are unnecessary, and consequently eyes and pigmentation are usually reduced or absent. To compensate for lack of vision, other traits, especially those related to chemo- and mechano-receptor sensations, are enhanced. Circadian rhythms that fine-tune organismal physiology with day-night cycles are also distorted, and light dependent behaviors, as well as the neural and endocrine circuits controlling these behaviors, are modified. Because photosynthetic organisms are not present in caves, primary productivity is absent and nutrient availability is usually limited. Survival under conditions of reduced and/or sporadic food resources is possible due to the evolution of modified feeding behaviors and adaptive changes in metabolism, such as lower metabolic rate, increased starvation resistance, and changes in carbohydrate and lipid metabolism [1].

The ancestors of cave dwelling animals originally lived on the surface. Regardless of whether the pioneering animals entered the subsurface accidently (by capture of surface waters or by falling into a pit) or purposely (to take refuge from harsh competition or changing climate conditions), they were suddenly exposed to darkness and subterranean living conditions. How did they overcome the challenges of life in darkness, such as orientation in the absence of light, survival during long periods without food, and detection of mates, in order to successfully establish underground lineages? The preadaptation hypothesis suggests that the ancestors of cave adapted animals were pre-adapted to darkness by already leading semi-nocturnal lifestyles in environments with low-light penetration, such as rotting logs, leaf litter, or in the soil, simplifying their transition to life in caves [3]. However, many cave dwelling animals, such as the cavefish *Astyanax mexicanus,* are descended from diurnal surface-dwelling animals with no obvious pre-adaptations to low light. For these animals, the transition to dark subterranean habitats posed significant challenges.

In the present investigation, we used the teleost *Astyanax mexicanus* as a model system to understand the molecular, physiological and morphological basis of cave colonization. *A. mexicanus* is an excellent system for studying adaptation to cave life because it consists of both the ancestral-proxy form and multiple derived forms: surface dwelling (surface fish, SF)

and cave-dwelling conspecifics (cavefish, CF) respectively. Surface fish live in rivers exposed to day-night cycles with abundant food availability. In the karstic Sierra Madre Oriental del Norte mountain range in Mexico, SF have colonized about 30 caves [4], and their cave dwelling descendants have adapted to permanently dark, mostly food restricted subterranean waters.

Recent studies revealed that cavefish lineages are much younger than previously thought, from less than 20,000 [5] to about 200,000 [6] years old, implying that the evolution of numerous cave-related phenotypes may have occurred over relatively short time periods. Furthermore, troglomorphic phenotypes are maintained in *A. mexicanus* cavefish despite the lack of complete isolation between surface fish and cavefish populations [6–9]. A remarkably recent origin of troglomorphic traits, also involving likely immigration from surface populations, has also been proposed for the evolution of cave-related traits in other cave dwelling animals, including invertebrates and vertebrates [10–15]. What are the mechanisms that enable the rapid evolution of various distinct cave-related phenotypes, and how are they preserved despite the homogenizing process of gene flow from surface populations? Clearly, strong selection must be involved in these cases, but in order for selection to act, it is essential to have phenotypic variants with differences in fitness in the cave environment.

The conspecific surface and cave morphs of *A. mexicanus* are capable of hybridization in the laboratory and thus have been the subjects of extensive genetic analysis [16–18]. However, not many mutations have been uncovered in CF, even in the presumably dispensable genes associated with eye degeneration, such as crystallin genes [19,20]. A more immediate mechanism for survival is likely necessary when new colonizers first enter caves. This suggests the presence of standing genetic variation and/or phenotypic plasticity followed by genetic assimilation [21], rather than the complete reliance on the accumulation of new mutations to produce the necessary variability. An instance of standing genetic variation has been reported in *A. mexicanus* CF with respect to the evolution of eye reduction [22], but phenotypic plasticity has not been studied extensively in this system (but see [23]). This is surprising since phenotypic plasticity plays an important role in the adaptation of many different organisms to changing environments and the colonization of new habitats (reviewed in 24,25).

To replicate the colonization of the subterranean environment, we placed *A. mexicanus* SF in completely dark conditions for up to two years. By assaying different traits, we discovered that dark-raised SF show numerous phenotypes that are normally associated with CF adaptations to dark environments. The results imply that some cave-adapted traits may have appeared rapidly by phenotypic plasticity in *A. mexicanus*. Our results provide a basis for the evolution of adaptations in the cavefish lineage by genetic assimilation

MATERIALS AND METHODS

Animals and Experimental Conditions

The study groups included *Astyanax mexicanus* SF and CF primarily from Pachón Cave (PA). In some experiments, CF from Tinaja (TI) and Molino (MO) caves were also used. Animals were obtained from the Jeffery Laboratory colony at the University of Maryland, and had undergone 3-5 generations in captivity since their original collection from the caves in 2002 (PA, TI) or 2006 (MO). Spawning was induced by an episode of extra feeding and an increased temperature regime [26]. The fish were raised and handled according to established University of Maryland and NIH guidelines.

Fish were initially exposed to darkness either as embryos or young fry and then raised in the absence of light for up to two years. Embryos spawned at the same time were separated into two study groups: one group was kept in complete darkness (D/D) and the other group in a normal 14-hour light/10-hour dark photoperiod (L/D) beginning at different times from 1-2 hours to 3 days after spawning. All other conditions were identical between the D/D and L/D study groups. Fish were reared in 1, 3 or 7 liter plastic tanks with no filtration or running water. Water was changed periodically (at least once a month), and at the same time for every tank in the experiment. Fish were fed the same amount of brine shrimp once per day. Dim red light (25 watts) was used when it was necessary to feed or handle the fish in the dark. Fish groups of the appropriate age were used on a per experiment basis. Fish used in a single experiment were collected for analysis at approximately the same time on the same day. Dead fish were removed when they were observed.

For the F1 generation experiments, SF placed in D/D as embryos and raised for 2 years were spawned using standard procedures [26]. The spawned embryos (dSF) were divided in two groups within the first 24 hours post-fertilization, and one group was left in D/D conditions and the other group was placed in L/D photoperiod within first 24 hpf. A control group of SF spawned from L/D raised parents was also divided into two groups and raised in L/D or D/D during the period of experimentation.

The following procedure was used for collecting, and when necessary pulverizing, adult fish for the respective experiments: fish were sacrificed with 0.4 or 0.5 mg/L MS222, tricaine methanesulfonate (Western Chemical Inc., Ferndale, WA, USA). Fish were maintained in the dark until they expired and then photographed, weighed, and pulverized in liquid nitrogen using a mortar and pestle. The pulverized material was divided into several Eppendorf tubes and stored at -80˚C until further processing. For the brain chemistry experiment, whole brains were rapidly removed, placed in 1.5 mL Eppendorf tubes, immediately frozen on dry ice and stored at -80˚C until analysis.

Morphological Analysis

After photography, the body length (total: rostrum to tail tip, fork: rostrum to tail fork, and standard: rostrum to beginning of the tail), the dorsal-central width of the body (at the level of the operculum and at the beginning of the dorsal fin), the eye diameter, and the pupil diameter of 8 fish from each D/D and L/D experimental condition were measured using ImageJ software.

Five fish from each group, kept under the experimental conditions described above for 9 months, beginning 2 hours post fertilization (hpf) were used for melanophore quantification. Fish were fixed for 1 hr in 4% paraformaldehyde, washed three times in PBS, and examined under a stereomicroscope. Pigment cells were counted in four different places on the left side of each fish: in the proximal tail fin stripe, below the dorsal fin, along the dorsal flank of the trunk, and on the chin. Eyes of four SF kept in D/D and three L/D controls kept in experimental conditions for 1.5-2.5 years were embedded in paraplast blocks, sectioned, stained, and morphometric analyses was performed on retinal layers (following [17]).

RNA Sequencing, Differential Expression Analysis, and Identification of Enriched Pathways

Three surface fish kept in D/D and three in L/D experimental conditions for 7 months post-fertilization were used for RNA sequencing. Prior to RNA extraction, the stomach and liver were removed from the fish because they compromised RNA quality. Total RNA was isolated from samples stored in TRIzol reagent according to the manufacturer's instructions (Invitrogen, Carlsbad, CA, USA). The fragment size, concentration, RNA integrity number (RIN) and 28S/18S ratio of RNA extracts were determined using an Agilent 2100 Bioanalyzer (Agilent, Santa Clara, CA, USA). The cDNA libraries were constructed using TruSeq mRNA Library Prep Kit (Illumina, San Diego, CA, USA). Fragment sizes and concentrations of libraries were verified using an Agilent 2100 Bioanalyzer and ABI StepOnePlus Real-Time PCR machine (Thermo Fisher Scientific, , Waltham, MA, USA). The samples were sequenced in a single Hiseq X-ten lane with a strategy of 150 bp paired-ends (PE), resulting in about 8 Gb raw data for each sample. To avoid potential adapter contamination, the last 60 bp of all reads were trimmed. Subsequently, the reads were removed if they contained: 1) more than 50% low quality (Q<35) bases; 2) more than 10 Ns, and 3) were PCR duplications. Cleaned read quality was confirmed in FASTQC [27], and a total of 230,437,086 cleaned reads were retained for transcriptomic analysis. The reads have been submitted to NCBI SRA (accession numbers provided upon acceptance).

A local database was built on the Carbonate Cluster implemented by the National Center for Genome Analysis Support [28] using the *Astyanax mexicanus* draft genome v102.93 (GCA_000372685.1) and associated gene model annotation files. The index of the reference genome was built using Bowtie2 v2.3.2 [29], and paired-end clean reads were aligned to the reference genome using TopHat v2.1.1, with max-intron-length set to 1000 [30]. Transcript coverage and differential expression were determined following the Cufflinks pipeline [31]. Briefly, mapped reads for each sample were assembled using Cufflinks v2.1.1 with the parameters --frag-bias-correct, --multi-read-correct, --upper-quartile-norm, and --

compatible-hits-norm. Transcripts were merged using default Cuffmerge parameters, and Cuffquant with --frag-bias-correct and --multi-read-correct was implemented to quantify transcript expression. Significant changes between transcripts were calculated using Cuffdiff [32] with parameters --compatible-hits-norm, --frag-bias-correct, and --multi-read-correct for light and dark treatments. Results were visualized using the package CummeRbund [33] implemented in R.Studio v1.0.136 [34](Rstudio Team, 2015) using R v3.5.1 [35] (R Core Team, 2018).

Significantly differentially expressed genes ($p_{adj}<0.1$) were subjected to Gene Ontology (GO) and Kyoto Encyclopedia of Genes and Genomes (KEGG) pathway enrichment analysis as implemented on DAVID Bioinformatics Resources [36,37] (Huang et al., 2009a; Huang et al, 2009b) and pathways were investigated more closely using Reactome [38].

Real Time Quantitative RT-PCR

Total RNA was isolated from 10 to 12-month old adult SF and PA placed in D/D or L/D conditions within the first few hours after fertilization. After the liver and stomach were removed, the RNA from the remaining body was isolated with Trizol Reagent (Thermo Fisher Scientific, Waltham, MA, USA) according to the manufacturer's instructions and treated with DNAse to remove genomic DNA if present. Equal amounts of RNA (1.5 µg) were reverse transcribed using Superscript III or IV (Invitrogen, NY, USA). The cDNA concentration was adjusted to 12.5 ng/µL and up to 50 ng were used in each reaction. We tested 12 different HKG (housekeeping genes): (*ube2a*, *rpl13a*, *eef1a1l1*, *nek7*, *tbcb*, *rnf7*, *rpl27*, *ndufa6*, *ap5s1*, *mob4*, *lsm12a*, *actc1b*) using RefFinder, which is located on the Cotton EST Database webpage [39], and integrates currently available major computational programs (geNorm, Normfinder, BestKeeper, and the comparative ΔΔCt method) to compare and rank the candidate reference genes. The geometric mean of the 3 most stable HKG (*tbcb*, *mob4* and *rnf7*) was used for normalization. Primers for genes of interest were designed across exon/intron boundaries except for *pdx1*, where this was not possible (Supplementary Table 1). Primer efficiencies were calculated in Excel from standard curves, and those with efficiencies between 90 and 110% were used for quantifications. The resulting PCR products were sequenced to confirm the targeted genes. Relative expression was calculated according to a formula $\Delta Ct = E \wedge^{(Ct\ reference - Ct\ target)}$ (E = 1+primer efficiency/100) which enables the comparison of normalized expression of a gene between multiple samples, instead of ratios between two samples, taking primer efficiency into account. Statistical significance of observed expression differences was calculated by ANOVA and adjusted by Bonferroni index.

Starvation Resistance Determinations

SF and PA embryos were placed in L/D vs. D/D experimental conditions within 24 hpf. At 7 dpf (days post fertilization), the first day larval fish were fed brine shrimp, a group of 36 larvae from L/D and 36 from D/D per fish type was fed. Groups of 36 larvae from each experimental condition and each fish type were not fed. The fish were identically treated in

all other aspects, and the number of living fish was recorded daily. Dead fish were removed each day.

Statistical analyses for survival analysis were carried out using R version 3.5.3 (R Core Team, 2019). Differences in starvation resistance were compared with a Cox proportional hazards model using the function coxph() from the R package 'survival' [40]. For the parental generation, the model included the covariates fish (PA vs. SF), light status (D/D vs. L/D), and fish x light status. For the F1 generation, the model included the covariates fish (dSF vs. SF), light status (D/D vs. L/D) and fish x light status. If the null hypothesis that all $\beta = 0$ was rejected, *post-hoc* pairwise comparisons of contrasts were carried out using the function glht() from the package multcomp with the specification mcp = "Tukey" [41]. Proportionality assumptions for Cox proportional hazards models were tested using the coxphz() function [40].

Metabolic Rate Determinations

Unhatched SF and PA embryos or 7 dpf larvae were placed individually in air-tight glass vials filled to the top with fish system water that contained no air bubbles. Half of the vials from each type were kept in L/D and the other half were wrapped in aluminum foil and kept in the same way in D/D. After two days, the O_2 remaining in each vial was measured using a Membrane Inlet Mass Spectrometer (MIMS) Machine (Bay Instruments, Easton, MD, USA). The amount of O_2 consumed per fish was calculated by subtracting the measured amount of O_2 in the vials with fish from the mean amount of O_2 measured in blank vials without fish. This experiment was repeated twice with embryos and once with larvae. The same methods were used in all replications. For embryos, N = 18 (SF L/D), 19 (SF D/D), 18 (PA L/D), 25 (PA D/D), and for larvae, N = 20 (SF L/D), 24 (SF D/D), 20 (PA L/D) and 24 (PA D/D).

Cortisol Quantification

We quantified cortisol from adult SF (N = 4) and PA (N = 4) that were maintained in D/D or L/D experimental conditions for 1.5 to 2 years beginning before 3 dpf. Cortisol was extracted using previously developed procedures [42,43]. Briefly, tissue samples stored at -80˚C were thawed and homogenized in PBS after which 5 mL of diethyl ether was added. Following centrifugation for 5 min at 3500 x g, the cortisol-containing top layer was removed and evaporated in a fume hood overnight. The cortisol was reconstituted in PBS overnight at 4˚C and quantified using the Cortisol ELISA Kit (Item № 500360, Cayman Chemical, Ann Arbor MI, USA) following the kit protocol. Cortisol samples from fish within each group were pooled and assayed in triplicate. The recorded absorbance was compared to a standard curve to determine the cortisol concentration, and each sample was standardized to protein concentration determined by Pierce BCA Protein Assay Kit (Thermo Fisher Scientific, Waltham, MA, USA).

Hormone Quantifications

Levels of growth hormone (GH) (CSB-E12121Fh) and thyroid stimulating hormone (TSH) (CSB-EQ02726Fl) were quantified by ELISA using commercially available kits from Cusabio (Wuhan, China). Adult SF kept in D/D for 1.5 years and PA kept in the experiment for almost 2 years were used. Three fish were used in each group, except for SF D/D in which 4 fish were used. For comparison of hormone levels between different populations, 3 to 4-month old SF (N=8), PA (N=5), TI (N=3), and MO (N=4) were used. The fish tissue was weighed, and 3 µl PBS/mg tissue was added to each sample. After two freeze-thaw cycles and homogenization, the homogenate was centrifuged at 5000 x g for 5 min at 4˚C. Equal volumes of supernatant from each fish type were pooled and immediately loaded on the plate, 50 µl per well, in triplicate. Assays were performed following the manufacturer's instructions and concentrations were determined according to the standard curve. Results were standardized to protein concentration as described above.

Triglyceride Quantifications

We used three fish from each population (SF, PA) and treatment (D/D, L/D) aged approximately 1 year. Pulverized fish were weighed and 20 µl per mg of 6% NP-40 (Abcam, Cambridge, UK) was added to each sample. Samples were heated to 80-100°C for 2-5 minutes, and the process was repeated 2-3 times. Insoluble material was removed by centrifugation for 2 minutes at 13,000 rpm, and equal volumes of supernatants from all samples of the same fish type were pooled and diluted 20x in ddH_2O before ELISA. For ELISA, 50 µL of each sample was assayed in triplicate using the Triglyceride Quantification Assay Kit (ab65336), (Abcam, Cambridge, UK) according to the manufacturer's instructions. Concentrations were determined from the standard curve and standardized to protein concentration as described above.

Serotonin Quantification

Brains were dissected from PA and SF kept in L/D or D/D experimental conditions for 1.5 to 2 years beginning at or before 3 dpf, and from adult SF (N=8), PA (N=5), TI (N=5), and MO (N=6) kept in the main fish system and HPLC was used to quantify serotonin levels. In addition, we quantified serotonin (5-HT) in samples of pooled 5 larvae (7 dpf) placed in the L/D or D/D experimental conditions within first few hours after fertilization, N=6 (SF L/D), 5 (SF D/D), 5 (PA L/D), and 4 (PA D/D). Serotonin and its metabolite, 5-hydroxyindoleacetic acid (5-HIAA), were analyzed using HPLC with electrochemical detection as described previously with minor modifications [44]. Brains were placed into 100 µL of sodium acetate buffer (pH 5.0) containing the internal standard alpha-methyl dopamine (αMDA; Merck & Co., Inc., Kenilworth, NJ). Fish bodies were placed in either 200 to 400 µL of acetate buffer containing αMDA based on the amount of tissue present. Both tissue types were disrupted by sonication using a 4710 Ultrasonic Homogenizer (Cole-Parmer Instrument Co., Chicago IL) and stored at -80°C. Prior to analysis, the sonicated brain samples were thawed, 4 µL of 1 mg/mL ascorbate oxidase (Sigma-Aldrich, St. Louis, MO, USA) was added to each sample and the samples were centrifuged at 17,000 g for 15 min. Fish body samples were treated the

same way except that the supernatant was centrifuged a second time through a 0.2 µm filter. The filtered supernatant was removed and a Waters Alliance e2695 separation module was used to inject 50 µL of the supernatant onto a C_{18} 4 µm NOVA-PAK radial compression column (Waters Associates, Inc. Milford, MA) held at 30°C. The initial mobile phase (pH 4.1) was prepared using 8.6 g sodium acetate, 250 mg EDTA, 14 g citric acid, 80 mg octylsulfonic acid, and 80 mL methanol in 1 L of distilled water (monoamine standards and chemicals were purchased through Sigma-Aldrich) and adjusted with small additions of octylsulfonic acid, glacial acetic acid, and methanol to optimize the separation. Electrochemical detection was accomplished using an LC 4 potentiostat and glassy carbon electrode (Bioanalytical Systems, West Lafayette, IN, USA) set at a sensitivity of 0.5 nA/V (brain samples) or 1 nA/V (body samples) with an applied potential of +0.7 V versus an Ag/AgCl reference electrode. The pellet was solubilized in 400 µL of 0.4 N NaOH and protein content was analyzed using the Bradford method [45]. A CSW32 data program (DataApex Ltd., Czech Republic) was used to determine 5-HT and 5-HIAA concentrations in the internal standard mode using peak heights calculated from standards. Injection versus preparation volumes were corrected and amine concentrations were normalized by dividing pg amine by µg protein. Data were tested for differences using a Three Way Analysis of Variance (SigmaStat version 3.5, Systat Software Inc., San Jose, CA). In analyses that revealed a significant effect between groups, the Holm-Sidak method was used to conduct pairwise comparisons. All data were tested for the presence of outliers using the Grubb's test [46]. Based on this analysis two brain (PA D/D night, SF L/D day) and three body samples (PA D/D night, PA L/D day, SF D/D day) were deleted from the data set. In the end a total number of fish used in the analysis for brains was 9 (SF L/D day), 10 (SF D/D day), 10 (PA L/D day), 10 (PA D/D day), 7 (SF L/D night), 6 (SF D/D night), 4 (PA L/D night), 4 (PA D/D night) and for the bodies 10 (SF L/D day), 9 (SF D/D day), 8 (PA L/D day), 10 (PA D/D day), 7 (SF L/D night), 7 (SF D/D night), 4 (PA L/D night), 5 (PA D/D night).

The F1 offspring of Dark-raised Surface Fish

We measured metabolic rate and starvation resistance in the F1 offspring of dark raised (dSF) and control SF using the methods described above. Statistical analysis was also done using the methods described above. N=24 larvae per group in starvation resistance experiments and N=10 (L/D SF), 13 (D/D SF), 12 (L/D dSF) and 15 (D/D dSF) in metabolic rate experiments.

RESULTS

Morphological Changes in Dark-raised surface fish

In this study, we exposed SF to D/D from early developmental stages until up to 2 years after spawning, and compared them to L/D controls. As a first step we compared body shape, length and width, eye size, and pigmentation in SF raised under D/D and L/D conditions (Fig 1A). We found no consistent differences in body parameters or eye sizes between D/D and L/D SF (Fig 1B). However, when we histologically compared thickness of retinal layers between the two groups, 5 out of 7 layers were significantly different: D/D fish showed a thinning of the two plexiform layers and a thickening of the two nuclear layers and the photoreceptor layer (Fig 1D, Supplementary Fig 1). Surprisingly, we observed a significantly higher number of melanophores in the flank of the trunk and below the dorsal fin in D/D compared to L/D SF, although similar levels of pigmentation were noted in other regions of the body (Fig 1C).

Gene Expression Changes in Dark-raised Surface Fish

To understand the effects of exposure to constant darkness at the molecular level, a comparative transcriptomic analysis was conducted. We used three, 7 month-old surface fish placed in either D/D or L/D conditions within 1 dpf. RNA sequencing yielded 21.9 to 27.6 million reads from each fish, representing a total of 25,194 genes. Basic statistical data are included in Supplementary Table 2. We found 356 differentially expressed genes (DEG) at a significance threshold of $p_{adj}<0.1$ (Supplementary Table 3). Of these, 210 were up-regulated and 146 were down-regulated in the D/D fish; the set of DEGs contained 67 genes with unconfirmed functions. We were particularly interested in the genes related to known aspects of the CF phenotype. Genes involved in circadian regulation, locomotor rhythm and visual perception were down-regulated in D/D fish, whereas lipid metabolism was the main functional category enriched in the up-regulated gene set. Two genes involved in pigmentation were also changed but their expression was higher in D/D, consistent with the increase in pigment cells described above. We also found significant changes in gene expression which were not predicted from known CF-associated phenotypes. These genes function in oxidation-reduction processes, hormone activity, hemostasis, aromatic amino acid metabolism, gene expression, metabolism of proteins, and signal transduction (Fig 2).

To validate the RNAseq results, we examined the levels of several DEG by real time PCR (RT-PCR) (Fig 3). We confirmed the down-regulation of the hormone related genes *somatostatin 1 tandem duplicate 2* (*sst1.2*) and *inhibin beta B* (*inhbb*), ros involved *dual oxidase* (*duox*), the circadian rhythm genes *period circadian clock 2* (*per2*) and *cryptochrome-1-like* (*cry3b*), the vision related genes *retinoschisin 1a* (*rs1a*) and *tubby like protein 1a* (*tulp1a*), as well as genes involved in the regulation of metabolism *pancreatic and duodenal homeobox 1* (*pdx1*), and *deptor* in D/D compared to L/D SF. However, the tyrosine metabolism gene *hydroxyphenylpyruvate dioxygenase a* (*hpda*), and the tryptophan metabolism genes

tryptophan 2,3-dioxygenase (*tdo2a*), *aralkylamine N-acetyltransferase 1* (*aanat1*), and *tryptophan hydroxylase 1a* (*tph1a*) showed down-regulation according to RT-PCR results, whereas they were up-regulated in the transcriptome. This discrepancy may be related to differences in the age or condition of fish at the time of sampling.

In addition, we quantified some genes which did not show significant differential expression according to RNAseq results but are important for the cavefish phenotype: *heat shock protein 90α* (*hsp90aa1.2*), and the *de novo* DNA methyltransferases *dnmt1*, *dnmt3aa*, *dnmt3ab*, *dnmt3ba* and *dnmt3bb. Hsp90aa1.2, dnmt1* and *dnmt3bb* showed changes in expression related to photoperiod in *Astyanax*. The RNAseq results and subsequent RT-PCR validation showed changes in the expression of DEG relative to photoperiod in both SF and PA CF. Expression of some genes changed in the same direction in both SF and CF (e.g. *inhbb*, *per2*, *sst1.2*), whereas others changed in one and not the other fish type, or changed in the opposite directions in different fish types (e.g. *duox*, *nr1d1*, *tph1a*). Except for *duox* and *dnmt3bb.1*, all of the significantly changed genes show the same direction of changes in L/D vs. D/D SF and in SF vs. PA: *hsp90aa1.2*, *rs1a*, *tdo2a*, *dnmt1*, *per2*, *sst1.2*, *tulp1a*, *aanat1*, and *tph1a.*

Starvation Resistance in Dark-raised Surface Fish

A major challenge facing animals that colonize caves is low food availability due to limited or absent primary productivity. To determine how a surface ancestor may have coped with this difficulty, we raised SF and PA larvae in D/D and L/D beginning <24 hours post fertilization (hpf), without feeding (N=36 larvae/group). D/D and L/D controls were fed daily portions of brine shrimp from 7 dpf, when larvae normally lose their reliance on yolk and begin feeding. By 15 dpf, about 25% more SF and over 65% more PA unfed larvae were alive in D/D compared to L/D conditions. By 18 dpf, only a few unfed embryos were still alive, and they were all from the D/D conditions (8 PA and 2 SF) (Fig 4). The results also show that PA larvae survive starvation better than SF larvae regardless of the lighting conditions.

Metabolic Rate Decrease in Dark-raised Surface Fish

We hypothesized that fish in D/D survived starvation longer because of lower energy expenditure. To test this possibility, we measured O_2 consumption in SF exposed to D/D vs. L/D conditions within first 24 hpf and compared the results to PA larvae subjected to the same conditions. The results showed that SF and PA larvae raised in D/D have decreased metabolic rates when compared to SF and PA larvae raised in L/D conditions. This result was found to be significant in SF each time this experiment was conducted (3 replicates) for both 2.5 and 7.5-day-old larvae. In contrast, D/D PA showed a decrease in O_2 consumption at 2.5 but not at 7.5 dpf when compared to larvae raised in L/D. In addition, PA and SF metabolic rates were not significantly different at 2.5 dpf, whereas at 7.5 dpf PA has a lower metabolic rate than SF larvae raised in L/D conditions. In summary, at 2.5 dpf metabolic rate is similar between SF and PA, and darkness causes it to be reduced in both types of fish. However, by

7.5 dpf the metabolic rate in PA is reduced compared to L/D SF, and PA do not show a plastic response to darkness, whereas at the same age SF metabolic rate is still affected by darkness (Fig 5).

Cortisol Increases in Dark-raised Surface Fish

We hypothesized that exposure to constant darkness may represent a chronic stressor and tested this possibility by comparing cortisol levels in both L/D and D/D SF and PA. Surface fish raised in D/D conditions had significantly higher cortisol levels than L/D SF (Fig 6). In contrast, PA did not show a significant change in cortisol levels after exposure to D/D. This result was confirmed in three biological replicates using fish of different ages and different periods of dark exposure.

Fat Increase in Dark-raised Surface Fish

Our RNAseq results show that genes involved in many aspects of fat metabolism are up-regulated in D/D versus L/D reared SF. To confirm this on a phenotypic level, we quantified triglyceride content in SF and PA raised to adulthood under D/D and L/D conditions. In fish raised under L/D conditions, PA had higher triglyceride levels than SF. Surface fish raised in D/D conditions had markedly higher triglyceride levels than L/D SF. Triglyceride levels in D/D PA were also higher than levels measured in L/D PA, although the difference is more modest than that observed for SF (Fig 7).

Hormone Levels Change in Dark-raised Surface Fish

Because of morphological changes in the pituitary and thyroid glands in dark raised SF [47] and differential expression of some of the genes associated with pituitary hormones (e.g. *sst1.2*, *inhbb*, *ghrl*) in the dark-raised SF transcriptome in our studies, we quantified the levels of pituitary hormones TSH and GH in SF and PA adults raised in either L/D or D/D conditions. TSH levels were lower in D/D SF ($p<0.05$) when compared to L/D SF. In contrast, TSH levels in PA raised in L/D and D/D conditions were similar, and PA had higher TSH levels than SF regardless of lighting conditions (Fig 8A). When TSH levels were compared between SF and three populations of CF, there was a trend for higher TSH levels in TI ($P=0.07$), but not MO ($P=0.16$), and TSH levels where significantly higher in PA (Fig 8B). The levels of GH were higher in both SF and PA raised in D/D conditions when compared to fish raised in L/D (Fig 9A). All three populations of CF had higher GH levels than SF (Fig 9B).

Serotonin Decrease in Dark-raised Surface Fish

According to the RNAseq analysis, the tryptophan metabolism pathway was significantly up-regulated in D/D versus L/D SF, while real time qPCR suggested lower expression of the *tdo2a*, *aanat1* and *tph1a* genes in dark–raised SF. Therefore, we compared serotonin (5-HT) levels in D/D and L/D SF and PA adults by HPLC. Since serotonin levels fluctuate according to a daily rhythm [48], samples for this assay were collected between 11 AM and 3 PM (day) or

11 PM and 3 AM (night) regardless of rearing conditions. Serotonin concentrations were lower in the brains (Fig 10A) and the bodies (Fig 10B) of D/D compared to L/D SF. Likewise, the 5-HT metabolite 5-HIAA was lower in the brain of D/D SF (Supplementary Fig 2). It was not possible to quantify 5-HIAA in the body because it was masked by several interfering peaks. Serotonin levels in the SF brain, but not the body, were significantly lower at night when compared to samples collected during the day. In PA brains collected during the day, 5-HT levels were lower in fish raised in D/D when compared to L/D conditions but 5-HT levels were similar in D/D and L/D brains at night. Modest, but significant, changes in body 5-HT were evident in PA with increases in D/D relative to L/D collected during the day, and the converse change occurred in bodies collected during the night. Serotonin levels were significantly lower in PA brains and bodies when compared to SF regardless of experimental conditions (D/D, L/D, day/night). Comparison of SF brain 5-HT with TI, MO and PA fish showed that all three cave populations have lower brain 5-HT (Fig 10C). In contrast to adults, 5-HT was significantly higher in PA compared to SF at 7 dpf, and darkness did not affect 5-HT levels in either larval fish types (Fig 10D).

Progeny of Dark Raised Surface Fish Show Plasticity in Starvation Resistance and Metabolic Rate

To test whether the plastic changes in the fish reared in the dark during the first generation are maintained and transferred to the next generation, we induced spawning in D/D reared SF. In these fish, spawning occurred early in the morning, the normal time for CF spawning, in contrast to SF, which spawn early in the night. We measured starvation resistance and metabolic rate in F1 embryos (dSF) developing in D/D or in L/D during the second generation, as well as the offspring of L/D reared controls exposed to L/D or D/D conditions. The F1 larvae reared in L/D showed no differences in starvation resistance (Fig 11) or metabolic rate (Fig 12), regardless of whether they were the progeny of L/D or D/D parents. Their cohorts raised in darkness showed a modification in these phenotypes: dSF larvae derived from D/D parents showed slightly enhanced plasticity and a minor shift toward lower metabolic rate and higher starvation resistance (although not statistically significant) than larvae raised from L/D parents.

DISCUSSION

Our results show that exposure to constant darkness can trigger rapid changes in traits necessary for survival of *A. mexicanus* SF colonizers, which may have allowed for the adaptations evident in extant CF. These changes involve metabolic, neurological, morphological and molecular alterations via phenotypic plasticity. The initial plastic responses can be adaptive or non-adaptive. Subsequently, in the case of an adaptive response, plasticity will be further selected for, or in the case of non-adaptive or mal-adaptive responses selected against. Our findings strongly implicate phenotypic plasticity as an important mechanism and open the possibility for genetic assimilation as an underlying mechanism of cave colonization and adaptive evolution in *A. mexicanus.*

Phenotypic plasticity is often the first response of organisms exposed to an environmental change. The ability to quickly respond to novel environmental conditions is essential for initial survival and, eventually, for adaptation to occur on the genetic level [24,25,49]. Darkness is the initial stress new cave colonizers encounter: a hallmark of the subterranean realm, and the only environmental component shared by all underground habitats [2]. Building on the work of Rohner et al. [22], we hypothesized that stress may be an important facilitator of the rapid appearance of novel and beneficial traits that enabled ancestral SF to endure the environmental shift associated with their entry and ultimately their adaptation to life in perpetual darkness. To test our hypothesis, we used contemporary *A. mexicanus* SF as a proxy of the ancestral SF colonizers, and exposed them to complete darkness to simulate the most important condition that the original SF ancestors of CF experienced when colonizing caves. Indeed, we found an increase in cortisol level in D/D exposed SF supporting our initial premise of darkness activating a stress response.

We expected to find plastic changes in D/D reared SF involving pituitary and thyroid hormonal regulation, adipose tissue, and body shape based on the previous work on dark-raised *A. mexicanus* SF, Chica CF, and Los Sabinos CF [47]. Furthermore, experiments on *Poecillia mexicana*, another teleost with cave adapted lineages, showed that darkness caused degenerate changes in the spine and promoted sexual isolation between adjacent surface and cave lineages [50–52]. Although our study was unable to replicate the changes in body shape seen by Rasquin (1949), we confirmed her observation of the increase of body fat. We also confirmed changes in pituitary and thyroid hormone metabolism, both in gene expression and hormone levels. Down-regulation of *sst1.2*, a homologue of somatostatin - growth hormone-inhibiting hormone, is consistent with increased GH in D/D SF. In addition, the changes in TSH and GH levels we observed in dark raised SF are consistent with the reduction of basophils and the predominance of acidophils in the pituitary gland of D/D SF reported previously [47]. These results suggest that one of the immediate responses to cave colonization and darkness may be changes in the endocrine system. In fact, endocrine signaling is one of the molecular mechanisms involved in regulating plastic responses. Other molecular mechanisms underlying phenotypic plasticity include epigenetic changes, heat

shock proteins, and transcriptional regulation [53–55]. Our transcriptome analyses revealed that genes and GO terms involved in all of the above processes showed significant changes in response to darkness. In addition to hormonal signaling, there are changes in genes involved in the stress response, several different signal transduction pathways, protein metabolism including protein folding and posttranslational modifications, and genes showing transcription factor or epigenetic regulator activities. Furthermore, using RT-PCR we investigated additional genes known to control CF phenotypes, e.g. heat shock proteins and epigenetic regulators [56]. We found that the expression of *hsp90aa1.2*, *dnmt1* and *dnmt3bb* was changed in D/D SF. These results suggest that multiple molecular mechanisms underlying phenotypic plasticity may be mobilized by exposure of SF to darkness.

Our RNAseq results contained functional categories enriched in both the up- and the down-regulated dataset: hormone activity (as mentioned above) and oxidation-reduction processes. Changes in oxidation-reduction processes may be related to increased stress following the exposure to a changed environment. Alternatively, these changes may be light-dependent since light activates the production of reactive oxygen species (ROS) which, in turn, act as messengers between photoreception and the circadian clock [57,58]. Pathways involved in the response to oxidative stress, photoreception, and circadian regulation were down-regulated. Thus, the absence of light may directly reduce ROS production, photoreception, and circadian control by modifying a single signaling cascade.

Our study revealed many traits that change in SF upon exposure to darkness. Strikingly, all these traits are associated with the cave lifestyle, and almost all of them change to resemble CF adaptive phenotypes. For example, compared to SF, CF have higher starvation resistance [59], lower metabolic rate [60,61], higher basal cortisol level [43], lower serotonin levels (but see 62), and spawn later in the night (our observations). When exposed to darkness, in addition to mimicking higher GH and triglyceride levels in CF (see above), we found that SF show higher starvation resistance, lower metabolic rates, higher cortisol levels, lower serotonin levels, and spawn later in the night. The results demonstrate that for these traits SF begin to resemble CF in the same generation following exposure to complete darkness. Because these phenotypes are genetically determined and irreversible in CF, our results imply that the initial darkness-induced plastic responses in SF during a cave colonization event may have become fixed in the CF-like descendants via genetic assimilation. However, not all CF traits could be replicated by exposing SF to darkness. Therefore, although important, plasticity caused by constant darkness is not the only path for the appearance of cavefish traits. Other mechanisms, including plasticity caused by environmental factors other than darkness (e.g. changes in nutrient availability), standing genetic variation, new mutations, or any combination of these processes, might also be involved.

Although darkness is an ecologically relevant cue, the induction of changes in SF by the absence of light does not necessarily imply that they are adaptive for cave life. Plasticity can result in adaptive, non-adaptive as well as maladaptive responses [63,64]. It is easy to

understand how increased triglyceride content, starvation resistance or decreased metabolic rate can increase fitness in the (food-limited) cave environment, but the effects of neurotransmitter or hormone changes are less intuitive. Therefore, we hypothesized that, if a trait is adaptive, it would be present in multiple independently evolved cavefish populations. As a proof of principle, higher starvation resistance and triglyceride content [59] conform to this criterion. We tested neurotransmitter and hormone levels and showed that GH and serotonin change in multiple CF concordantly to the initial SF plastic response. Conversely, TSH showed the opposite direction of changes suggesting that the initial SF plastic response was not adaptive.

In addition to TSH levels which decrease, melanophore numbers increase in D/D SF, which is opposite to the respective traits expressed in CF. The increase in melanophores in dark-raised SF was modest and confined to specific regions of the body, but consistent with up-regulation of some melanosome-related genes in the transcriptome. This result was unexpected but considered reliable, since SF x CF hybrids can also show hyper-melanization [65], and neutral mutations are a likely cause of melanophore reduction in *A. mexicanus* CF [66]. We found a surprising result in another classic troglomorphic trait, eye degeneration: although visual perception was a GO term associated with down-regulated DEGs in D/D SF transcriptome, we were unable to detect changes in eye size. However, D/D SF exhibited well-developed retinal layers, and we even recorded thickening of the inner and outer nuclear layer, and the photoreceptor layer. These regions are cell proliferation and intercalation centers so it is possible that darkness activates mitotic activity in these retinal layers as a compensation for defective transmission of light from the lens and induced retinal stress [67]. Our results nicely exemplify how plasticity does not have the propensity to produce adaptive variants, and non-adaptive, even maladaptive, effects seem to be as likely as adaptive outcomes. Although the initial plastic responses may be random, our study further demonstrates that they may direct the subsequent course of evolution (see later).

Most of the plastic traits still show sensitivity to darkness in CF (e.g. GH, starvation resistance, metabolic rate; and triglyceride levels), but the magnitude of response is smaller than in SF. However, some traits have completely lost plasticity in CF, such as TSH levels and in particular pigmentation and eyes, which are completely absent in Pachón and other fully troglomorphic CF. The process of replacing a plastic trait by a monomorphic trait desensitized from environmental stimuli is called canalization [68]. Our results suggest that different traits can have different extents of canalization during the evolution of CF, implying that the rate of canalization is not proportional to the time lapse since colonization of the new habitat. The loss of plasticity may be a consequence of drift because a phenotype is never expressed in a derived environment or it can be adaptive if maintenance of plasticity is costly or only one phenotype is favored in the environment [69]. Importantly, the three traits that have been completely canalized in CF, showed plastic response in SF that was non-adaptive or potentially maladaptive. This suggests that natural selection acting against plasticity was involved in the evolution of these traits in CF. A novel aspect of the evolution

of classical troglomorphic traits, the reduction of eyes and pigmentation, may be that they are partly a consequence of strong selection against non- or mal-adaptive plastic responses during colonization of caves by surface ancestors.

To test if the inheritance of some of the plastic phenotypic changes described here occur during the next generation, we induced spawning in D/D SF and investigated starvation resistance and metabolic rate in the offspring (dSF), traits shown to exhibit plasticity in the parental D/D generation. Neither of these traits showed changes between offspring spawned in the light or dark when maintained in L/D. However, when maintained in D/D, dSF offspring showed increased plasticity and a minor shift in tested characters towards their refinement. Therefore, no genetic assimilation of the plastic response took place. Conversely, we detected continued and enhanced plasticity of both traits as well as a potential adaptive-tuning of the character states in the second generation. The latter suggests that plasticity is evolvable and can be an evolutionary adaptation itself. Increased plasticity was previously suggested to be an important stepping stone in the process of adaptations to extreme environments [49,70]. Therefore, consistent with the Baldwin effect [71], the evolution of cave related traits may have proceeded through initial selection for continued plasticity and refinement of the characters, followed by selection of individuals carrying the most improved variants of the phenotype. Higher growth hormone and triglyceride levels, as well as lower body serotonin levels in PA than D/D SF, also imply refinement of the initial SF plastic response in CF.

One of the reasons the role of plasticity in the adaptive evolution has been contested is its randomness in the production of outcomes where non-adaptive and mal-adaptive responses are as likely as adaptive responses. However, our study suggests that even the initial non-adaptive plastic responses may in the end produce an adaptive outcome. Some traits, including the hallmarks of troglomorphic adaptations (the loss of eyes and pigmentation) initially show non-adaptive plastic responses but the complete canalization of the opposite character state in CF indicates strong selection against plasticity in SF colonizers. Non-adaptive plasticity may have a greater role in evolution than previously appreciated because it may increase the strength of selection against plasticity, and perhaps, in some cases, may affect the whole trait itself. Conversely, in cases where plasticity produces adaptive outcomes, initial selection will act to enhance plasticity, and plasticity will be maintained in the derived lineage for many generations. Overall, plasticity has a critical role in producing variability (adaptive or not) on which selection can act (for or against) to produce individuals with optimal fitness in the new environment.

We also uncovered two cases in which the plasticity of a single trait changes within an individual over the course of development. Both metabolic rate and serotonin showed shifts in plasticity depending on developmental stage. Metabolic rate initially (at 2.5 dpf) changes in response to the light regime but by 7.5 dpf this response is lost in PA. In contrast, serotonin levels are plastic in adults but not in 7 dpf larvae. Interestingly, switches in

plasticity occur at the same time as switches in character state. At 2.5 dpf there is no difference in metabolic rate between SF and PA, but by 7.5 dpf, the metabolic rate in PA is lower than in SF, agreeing with previous studies done on adults [60,61]. In the case of serotonin, character states show opposite relationships at different stages: they are lower in larvae but higher in adult SF compared to PA. Therefore, for metabolic rate and serotonin levels, both the trait and its plasticity change concordantly, suggesting that the underlying mechanisms of character development may also influence the ability to respond to environmental stimuli. These two examples show that plasticity is not an intrinsically fixed property of a trait but can develop by itself. In our examples, plasticity develops concordantly with the traits it affects, and it can develop in a direction of expansion or reduction. The development of metabolic rate in PA is accompanied by canalization of the same trait. In the case of serotonin, development of the 5-HT system is accompanied by an increase in its plasticity.

There are several open questions about the current model of cave colonization and the evolution of cave dwelling organisms: how did non-adapted surface ancestors survive the extreme conditions of the subterranean realm, how was it possible to evolve numerous adaptations to a novel environment within a very short timeframe, and how were such adaptations maintained in the face of gene flow from the ancestral population. Our results suggest that phenotypic plasticity can fill all of these gaps. First, although not yet adapted, the colonizing surface ancestor could have survived the extreme subsurface environment because darkness elicits plastic responses in many traits necessary for survival. Phenotypic plasticity may also be a facilitator of “pre-adaptation” (when it occurs), which enabled a surface ancestor to simplify the transition between two very different environments. Second, it is possible to evolve numerous adaptations within a very short timeframe; in fact, adaptive traits can arise within a single generation via phenotypic plasticity. Finally, plasticity may enable the maintenance of distinct phenotypes in the face of gene flow from conspecific surface-dwelling populations.

ACKNOWLEDGEMENTS

This research was supported by NIH grant EY024941 to WRJ. HB was supported from the European Union Seventh Framework Programme (FP7 2007-2013) under grant agreement no. 291823 Marie Curie FP7-PEOPLE-2011-COFUND – NEWFELPRO as part of the project EACAA, grant agreement No. 50. MP and MS were supported by NSF grant #1556819. We wish to thank all members of the Jeffery lab, especially Ruby Dessiatoun for taking care of the fish.

REFERENCES

1. Culver DC, Pipan T. The biology of caves and other subterranean habitats. USA: Oxford University Press; 2009.

2. Pipan T, Culver DC. Convergence and divergence in the subterranean realm: a reassessment. Biol J Linn Soc. 2012; 107: 1–14. Available: http://onlinelibrary.wiley.com/doi/10.1111/j.1095-8312.2012.01964.x/full

3. Vandel A. Biospeleology: the biology of cavernicolous animals. Pergamon Press; 1965.

4. Gross JB. The complex origin of *Astyanax* cavefish. BMC Evol Biol. 2012; 12: 105. doi:10.1186/1471-2148-12-105

5. Fumey J, Hinaux H, Noirot C, Thermes C, Rétaux S, Casane D. Evidence for late Pleistocene origin of *Astyanax mexicanus* cavefish. BMC Evol Biol. BioMed Central; 2018; 18: 43. doi:10.1186/s12862-018-1156-7

6. Herman A, Brandvain Y, Weagley J, Jeffery WR, Keene AC, Kono TJY, et al. The role of gene flow in rapid and repeated evolution of cave-related traits in Mexican tetra, *Astyanax mexicanus*. Mol Ecol. John Wiley & Sons, Ltd (10.1111); 2018; 27: 4397–4416. doi:10.1111/mec.14877

7. Chakraborty R, Nei M. Dynamics of gene differentiation between incompletely isolated populations of unequal sizes. Theor Popul Biol. Academic Press; 1974; 5: 460–469. doi:10.1016/0040-5809(74)90064-1

8. Bradic M, Beerli P, García-de León FJ, Esquivel-Bobadilla S, Borowsky RL. Gene flow and population structure in the Mexican blind cavefish complex (*Astyanax mexicanus*). BMC Evol Biol. 2012; 12: 9. Available: http://www.biomedcentral.com/1471-2148/12/9/

9. Wilkens H, Hüppop K. Sympatric speciation in cave fishes? J Zool Syst Evol Res. John Wiley & Sons, Ltd (10.1111); 1986; 24: 223–230. doi:10.1111/j.1439-0469.1986.tb00630.x

10. Behrmann-Godel J, Nolte AW, Kreiselmaier J, Berka R, Freyhof J. The first European cave fish. Curr Biol. Elsevier; 2017; 27: R257–R258. doi:10.1016/j.cub.2017.02.048

11. Niemiller ML, Fitzpatrick BM, Miller BT. Recent divergence with gene flow in Tennessee cave salamanders (Plethodontidae: Gyrinophilus) inferred from gene genealogies. Mol Ecol. 2008; 17: 2258–2275. doi:10.1111/j.1365-294X.2008.03750.x

12. Klaus S, Mendoza JCE, Liew JH, Plath M, Meier R, Yeo DCJ. Rapid evolution of troglomorphic characters suggests selection rather than neutral mutation as a driver of eye reduction in cave crabs. Biol Lett. 2013; 9. doi:10.1098/rsbl.2012.1098

13. Zhang Y, Li S. Ancient lineage, young troglobites: recent colonization of caves by *Nesticella* spiders. BMC Evol Biol. BioMed Central; 2013; 13: 183. doi:10.1186/1471-2148-13-183

14. Schilthuizen M, Cabanban AS, Haase M. Possible speciation with gene flow in tropical

cave snails. J Zool Syst Evol Res. John Wiley & Sons, Ltd (10.1111); 2005; 43: 133–138. doi:10.1111/j.1439-0469.2004.00289.x

15. Villacorta C, Jaume D, Oromí P, Juan C. Under the volcano: phylogeography and evolution of the cave-dwelling *Palmorchestia hypogaea* (Amphipoda, Crustacea) at La Palma (Canary Islands). BMC Biol. BioMed Central; 2008;6: 7. doi:10.1186/1741-7007-6-7

16. Protas M, Tabansky I, Conrad M, Gross JB, Vidal O, Tabin CJ, et al. Multi-trait evolution in a cave fish, *Astyanax mexicanus*. Evol Dev. 2008; 10: 196–209. doi:10.1111/j.1525-142X.2008.00227.x

17. O'Quin KE, Yoshizawa M, Doshi P, Jeffery WR. Quantitative genetic analysis of retinal degeneration in the blind cavefish *Astyanax mexicanus*. PLoS One. 2013; 8: e57281. Available: http://dx.plos.org/10.1371/journal.pone.0057281

18. Yoshizawa M, Yamamoto Y, O'Quin KE, Jeffery WR. Evolution of an adaptive behavior and its sensory receptors promotes eye regression in blind cavefish. BMC Biol. 2012; 10: 108. Available: http://www.biomedcentral.com/1741-7007/10/108/

19. Hinaux H, Poulain J, Da Silva C, Noirot C, Jeffery WR, Casane D, et al. De Novo sequencing of *Astyanax mexicanus* surface fish and Pachón cavefish transcriptomes reveals enrichment of mutations in cavefish putative eye genes. PLoS One. 2013; 8: e53553. doi:10.1371/journal.pone.0053553

20. Ma L, Parkhurst A, Jeffery WR. The role of a lens survival pathway including sox2 and αA-crystallin in the evolution of cavefish eye degeneration. EvoDevo. BioMed Central; 2014; 5: 28. doi:10.1186/2041-9139-5-28

21. Waddington CH. Genetic assimilation of an acquired character. Evolution. Society for the Study of Evolution; 1953; 7: 118–126. doi:10.2307/2405747

22. Rohner N, Jarosz DF, Kowalko JE, Yoshizawa M, Jeffery WR, Borowsky RL, et al. Cryptic variation in morphological evolution: HSP90 as a capacitor for loss of eyes in cavefish. Science. NIH Public Access; 2013; 342: 1372–5. doi:10.1126/science.1240276

23. Reyes WD. Via Sapientiae: Effects of temperature and water flow on morphology of *Astyanax mexicanus* (Teleostei: Characidae) [Internet]. 2015. Available: https://via.library.depaul.edu/csh_etd/112

24. Fox RJ, Donelson JM, Schunter C, Ravasi T, Gaitán-Espitia JD. Beyond buying time: the role of plasticity in phenotypic adaptation to rapid environmental change. Philos Trans R Soc B Biol Sci. The Royal Society; 2019; 374: 20180174. doi:10.1098/rstb.2018.0174

25. Morris MRJ. Plasticity-mediated persistence in new and changing environments. Int J Evol Biol. Hindawi; 2014; 2014. doi:10.1155/2014/416497

26. Jeffery WR, Strickler AG, Guiney S, Heyser DG, Tomarev SI. Prox 1 in eye degeneration and sensory organ compensation during development and evolution of the cavefish *Astyanax*. Dev Genes Evol. 2000; 210: 223–230. Available: http://link.springer.com/article/10.1007/s004270050308

27. Andrews S. FastQC: A quality control tool for high throughput sequence data. http://www.bioinformatics.babraham.ac.uk/projects/fastqc/. 2010.

28. Stewart CA, Welch V, Plale B, Fox G, Pierce M, Sterling T. Indiana University Pervasive Technology Institute [Internet]. 2017. doi:10.5967/K8G44NGB

29. Langmead B, Salzberg SL. Fast gapped-read alignment with Bowtie 2. Nat Methods. Nature Publishing Group; 2012; 9: 357–359. doi:10.1038/nmeth.1923

30. Kim D, Pertea G, Trapnell C, Pimentel H, Kelley R, Salzberg SL. TopHat2: accurate alignment of transcriptomes in the presence of insertions, deletions and gene fusions. Genome Biol. BioMed Central; 2013; 14: R36. doi:10.1186/gb-2013-14-4-r36

31. Trapnell C, Williams BA, Pertea G, Mortazavi A, Kwan G, van Baren MJ, et al. Transcript assembly and quantification by RNA-Seq reveals unannotated transcripts and isoform switching during cell differentiation. Nat Biotechnol. Nature Publishing Group; 2010; 28: 511–515. doi:10.1038/nbt.1621

32. Trapnell C, Roberts A, Goff L, Pertea G, Kim D, Kelley DR, et al. Differential gene and transcript expression analysis of RNA-seq experiments with TopHat and Cufflinks. Nat Protoc. Nature Publishing Group; 2012; 7: 562–578. doi:10.1038/nprot.2012.016

33. Goff LA, Trapnell C, Kelley D. CummeRbund: Visualization and Exploration of Cufflinks High-throughput Sequencing Data [Internet]. 2014. Available: https://www.bioconductor.org/packages/devel/bioc/vignettes/cummeRbund/inst/doc/cummeRbund-manual.pdf

34. R Studio T. RStudio: Integrated development environment for R [Internet]. Citeseer. Boston, MA; 2015. Available: http://www.rstudio.com/.

35. Team R. R: A language and environment for statistical computing. 2018; Available: ftp://ftp.uvigo.es/CRAN/web/packages/dplR/vignettes/intro-dplR.pdf

36. Huang DW, Sherman BT, Lempicki RA. Systematic and integrative analysis of large gene lists using DAVID bioinformatics resources. Nat Protoc. Nature Publishing Group; 2009; 4: 44–57. doi:10.1038/nprot.2008.211

37. Huang DW, Sherman BT, Lempicki RA. Bioinformatics enrichment tools: paths toward the comprehensive functional analysis of large gene lists. Nucleic Acids Res. Oxford University Press; 2009; 37: 1–13. doi:10.1093/nar/gkn923

38. Fabregat A, Sidiropoulos K, Garapati P, Gillespie M, Hausmann K, Haw R, et al. The Reactome pathway knowledgebase. Nucleic Acids Res. Oxford University Press; 2016; 44: D481–D487. doi:10.1093/nar/gkv1351

39. Xie F, Sun G, Stiller JW, Zhang B. Genome-wide functional analysis of the cotton transcriptome by creating an integrated EST database. PLoS One. Public Library of Science; 2011; 6: e26980. doi:10.1371/journal.pone.0026980

40. Therneau TM, Grambsch PM. Modeling Survival Data: Extending the Cox Model. New York, NY: Springer New York; 2000. doi:10.1007/978-1-4757-3294-8

41. Hothorn T, Bretz F, Westfall P. Simultaneous inference in Ggneral parametric models. Biometrical J. 2008; 50: 346–363. doi:10.1002/bimj.200810425

42. Canavello PRP, Cachat JMJ, Beeson EC, Laffoon AL AL, Grimes C, Haymore WAM, et al. Measuring endocrine (cortisol) responses of zebrafish to stress. In: Kalueff AV, Cachat J, editors. Zebrafish Neurobehavioral Protocols. Humana Press; 2011. pp. 135–142. doi:10.1007/978-1-60761-953-6_11

43. Gallo ND, Jeffery WR. Evolution of space dependent growth in the teleost *Astyanax mexicanus*. PLoS One. 2012; 7: e41443. doi:10.1371/journal.pone.0041443

44. Renner K, Luine V. Analysis of temporal and dose-dependent effects of estrogen on monoamines in brain nuclei. Brain Res. 1986; 366: 64–71. doi:10.1016/0006-8993(86)91281-3

45. Bradford MM. A rapid and sensitive method for the quantitation of microgram quantities of protein utilizing the principle of protein-dye binding. Anal Biochem. 1976; 72: 248–54. doi:10.1016/0003-2697(76)90527-3

46. Rohlf FJ, Soka RR. Statistical Tables [Internet]. 2nd ed. San Francisco: W.H. Freeman and Co; 1981. doi:10.1002/bimj.19700120315

47. Rasquin P. The influence of light and darkness on thyroid and pituitary activity of the characin *Astyanax mexicanus* and its cave derivatives. Bull Amer Mus nat Hist. 93: 497–528 New York : [American Museum of Natural History]; 1949; Available: http://digitallibrary.amnh.org/handle/2246/1190

48. Fingerman SW. Circadian rhythms of brain 5-hydroxytryptamine and swimming activity in the teleost, *Fundulus grandis*. Comp Biochem Physiol C. 1976; 54: 49–53. Available: http://www.ncbi.nlm.nih.gov/pubmed/6207

49. Lande R. Adaptation to an extraordinary environment by evolution of phenotypic plasticity and genetic assimilation. J Evol Biol. John Wiley & Sons, Ltd (10.1111); 2009; 22: 1435–1446. doi:10.1111/j.1420-9101.2009.01754.x

50. Riesch R, Plath M, Schlupp I. Speciation in caves: experimental evidence that permanent darkness promotes reproductive isolation. Biol Lett. 2011; 7: 909–912. doi:10.1098/rsbl.2011.0237

51. Riesch R, Reznick DN, Plath M, Schlupp I. Sex-specific local life-history adaptation in surface- and cave-dwelling Atlantic mollies (*Poecilia mexicana*). Sci Rep. 2016; 6: 22968. doi:10.1038/srep22968

52. Torres-Dowdall J, Karagic N, Plath M, Riesch R. Evolution in caves: selection from darkness causes spinal deformities in teleost fishes. Biol Lett. The Royal Society; 2018; 14: 20180197. doi:10.1098/rsbl.2018.0197

53. Beldade P, Mateus A, Keller R. Evolution and molecular mechanisms of adaptive developmental plasticity. Mol Ecol. Wiley/Blackwell (10.1111); 2011; 20: 1347–1363. doi:10.1111/j.1365-294X.2011.05016.x

54. Aubin-Horth N, Renn SCP. Genomic reaction norms: using integrative biology to understand molecular mechanisms of phenotypic plasticity. Mol Ecol. Wiley/Blackwell (10.1111); 2009; 18: 3763–3780. doi:10.1111/j.1365-294X.2009.04313.x

55. Kelly SA, Panhuis TM, Stoehr AM. Phenotypic plasticity: molecular mechanisms and adaptive significance. Comprehensive Physiology. Hoboken, NJ, USA: John Wiley & Sons, Inc.; 2012. pp. 1417–1439. doi:10.1002/cphy.c110008

56. Gore A V., Tomins KA, Iben J, Ma L, Castranova D, Davis AE, et al. An epigenetic mechanism for cavefish eye degeneration. Nat Ecol Evol. Nature Publishing Group; 2018; 2: 1155–1160. doi:10.1038/s41559-018-0569-4

57. Hirayama J, Cho S, Sassone-Corsi P. Circadian control by the reduction/oxidation pathway: catalase represses light-dependent clock gene expression in the zebrafish. Proc Natl Acad Sci U S A. National Academy of Sciences; 2007; 104: 15747–52. doi:10.1073/pnas.0705614104

58. Pagano C, Siauciunaite R, Idda ML, Ruggiero G, Ceinos RM, Pagano M, et al. Evolution shapes the responsiveness of the D-box enhancer element to light and reactive oxygen species in vertebrates. Sci Rep. Nature Publishing Group; 2018; 8: 13180. doi:10.1038/s41598-018-31570-8

59. Aspiras AC, Rohner N, Martineau B, Borowsky RL, Tabin CJ. Melanocortin 4 receptor mutations contribute to the adaptation of cavefish to nutrient-poor conditions. Proc Natl Acad Sci USA. National Academy of Sciences; 2015; 112: 9668–73. doi:10.1073/pnas.1510802112

60. Hüppop K. Oxygen consumption of *Astyanax fasciatus* (Characidae, Pisces): A comparison of epigean and hypogean populations. Environ Biol Fishes. 1986; 17: 299–308.

61. Moran D, Softley R, Warrant EJ. Eyeless Mexican cavefish save energy by eliminating the circadian rhythm in metabolism. Mistlberger RE, editor. PLoS One. Public Library of Science; 2014; 9: e107877. doi:10.1371/journal.pone.0107877

62. Elipot Y, Hinaux H, Callebert J, Launay J-M, Blin M, Rétaux S. A mutation in the enzyme monoamine oxidase explains part of the *Astyanax* cavefish behavioural syndrome. Nat Commun. Nature Publishing Group; 2014; 5: 3647. doi:10.1038/ncomms4647

63. Langerhans RB, DeWitt TJ. Plasticity constrained: over-generalized induction cues cause maladaptive phenotypes. Evol Ecol Res. Evolutionary Ecology; 2002; 4: 857–870.

64. Ghalambor CK, McKay JK, Carroll SP, Reznick DN. Adaptive versus non-adaptive phenotypic plasticity and the potential for contemporary adaptation in new environments [Internet]. Functional Ecology Jun 1, 2007 pp. 394–407. Available: http://doi.wiley.com/10.1111/j.1365-2435.2007.01283.x

65. Gross JB, Powers AK, Davis EM, Kaplan SA. A pleiotropic interaction between vision loss and hypermelanism in *Astyanax mexicanus* cave x surface hybrids. BMC Evol Biol. BioMed Central; 2016; 16: 145. doi:10.1186/s12862-016-0716-y

66. Protas M, Conrad M, Gross JB, Tabin C, Borowsky R. Regressive evolution in the Mexican cave tetra, *Astyanax mexicanus*. Curr Biol. 2007; 17: 452–454. doi:10.1016/j.cub.2007.01.051

67. Alunni A, Menuet A, Candal E, Pénigault J-B, Jeffery WR, Rétaux S. Developmental mechanisms for retinal degeneration in the blind cavefish *Astyanax mexicanus*. J Comp Neurol. 2007; 505: 221–233. doi:10.1002/cne.21488

68. Waddington CH. Canalization of development and genetic assimilation of acquired characters. Nature. Nature Publishing Group; 1959; 183: 1654–1655. doi:10.1038/1831654a0

69. Schwander T, Leimar O. Genes as leaders and followers in evolution. Trends Ecol Evol. 2011; 26: 143–151. doi:10.1016/j.tree.2010.12.010

70. Lande R. Evolution of phenotypic plasticity in colonizing species. Mol Ecol. 2015; 24: 2038–2045. doi:10.1111/mec.13037

71. Crispo E. The Baldwin effect and genetic assimilation: revisiting two mechanisms of evolutionary change mediated by phenotypic plasticity. John Wiley & Sons, Ltd (10.1111); 2007; 61: 2469–2479. doi:10.1111/j.1558-5646.2007.00203.x

FIGURES AND FIGURE LEGENDS

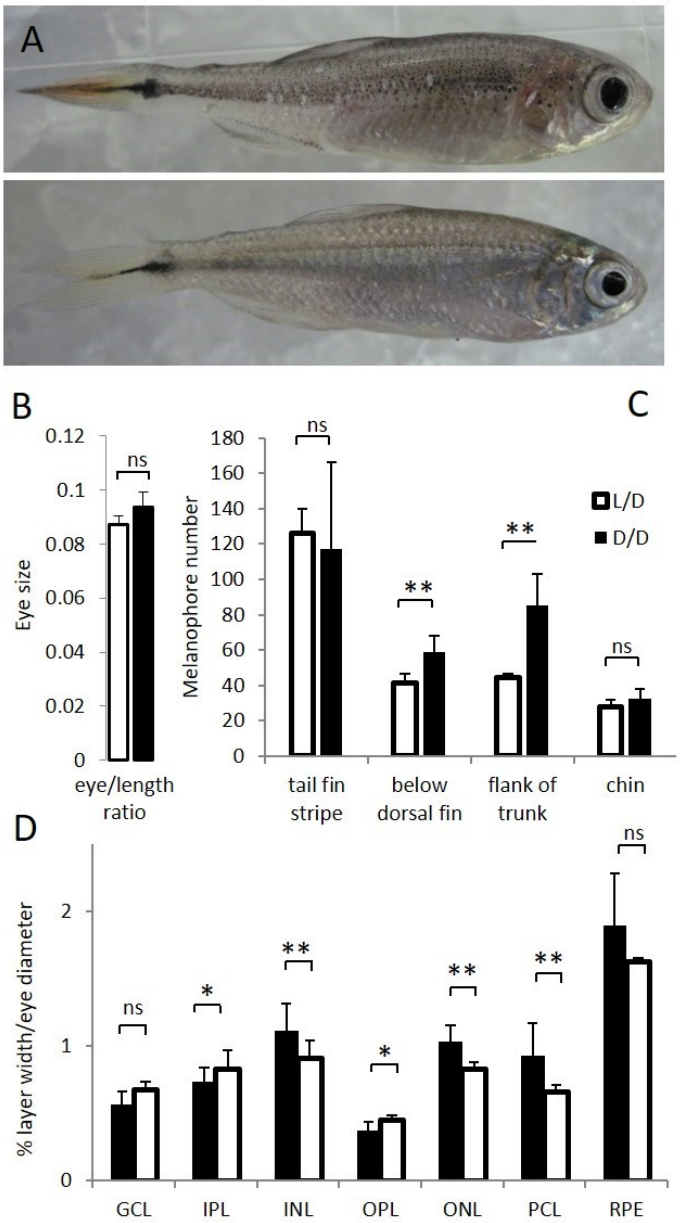

Figure 1. A. Surface fish (SF) kept in constant dark (D/D; top frame) vs. light/dark (L/D; bottom frame) photoperiod for 1 year. B. Eye size normalized by body length in D/D vs. L/D SF kept in the experimental conditions for 1 to 2 years. C. Number of melanophores in 1 year-old D/D vs. L/D SF determined in 4 different body regions. D. Thickness of retinal layers in D/D vs. L/D fish: GCL, ganglion cell layer; IPL, inner plexiform layer; INL, inner nuclear layer; OPL, outer plexiform layer; ONL, outer nuclear layer; PCL photoreceptor cell layer; RPE, retinal pigment epithelium measured as a ratio to eye diameter. (Error bars: SD; T-test Ns – not significant, *p<0.05, ** P<0.001).

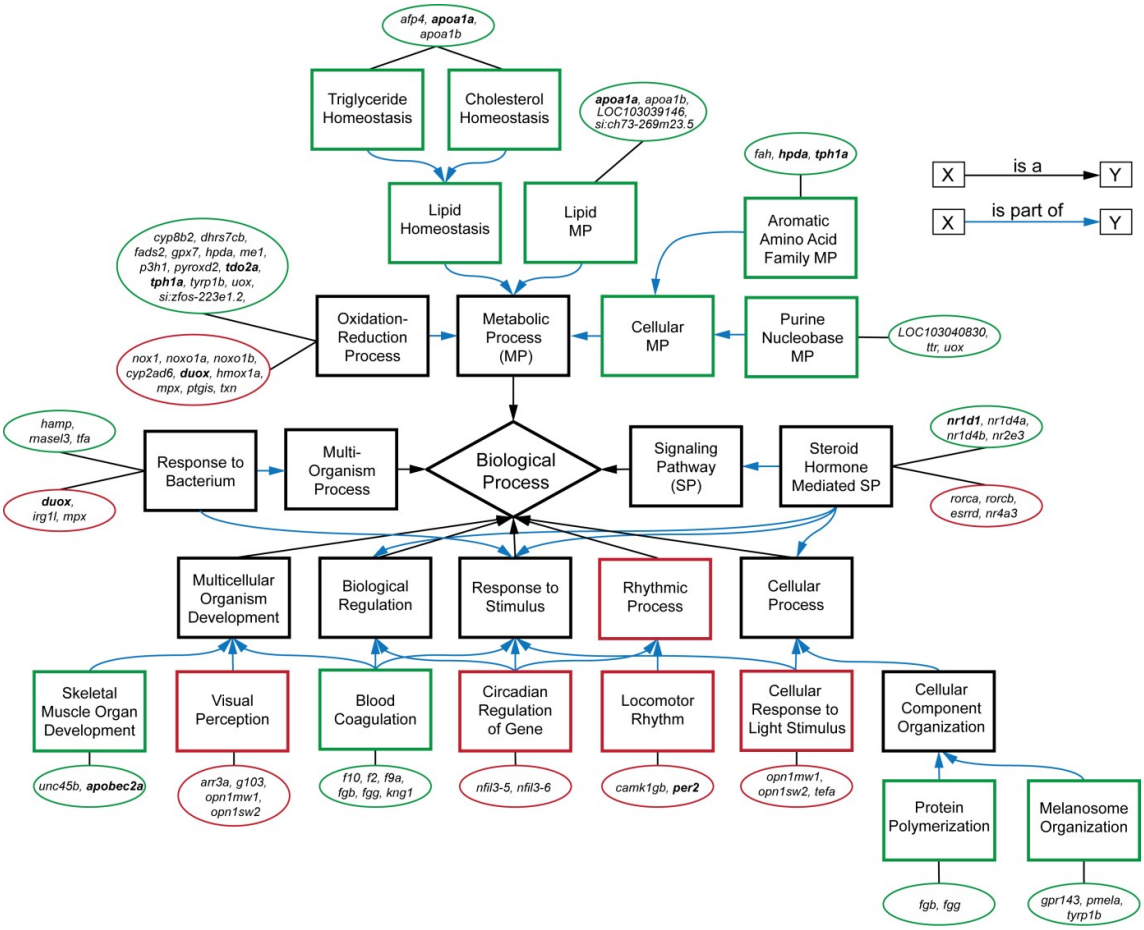
afp4, apoa1a, apoa1b
Triglyceride Homeostasis
Cholesterol Homeostasis
apoa1a, apoa1b, LOC103039146, si:ch73-269m23.5
fah, hpda, tph1a
X is a Y
X is part of Y
Lipid Homeostasis
Lipid MP
Aromatic Amino Acid Family MP
cyp8b2, dhrs7cb, fads2, gpx7, hpda, me1, p3h1, pyroxd2, tdo2a, tph1a, tyrp1b, uox, si:zfos-223e1.2,
Oxidation-Reduction Process
Metabolic Process (MP)
Cellular MP
Purine Nucleobase MP
LOC103040830, ttr, uox
nox1, noxo1a, noxo1b, cyp2ad6, duox, hmox1a, mpx, ptgis, txn
hamp, masel3, tfa
Response to Bacterium
Multi-Organism Process
Biological Process
Signaling Pathway (SP)
Steroid Hormone Mediated SP
nr1d1, nr1d4a, nr1d4b, nr2e3
duox, irg1l, mpx
rorca, rorcb, esrrd, nr4a3
Multicellular Organism Development
Biological Regulation
Response to Stimulus
Rhythmic Process
Cellular Process
Skeletal Muscle Organ Development
Visual Perception
Blood Coagulation
Circadian Regulation of Gene
Locomotor Rhythm
Cellular Response to Light Stimulus
Cellular Component Organization
unc45b, apobec2a
arr3a, g103, opn1mw1, opn1sw2
f10, f2, f9a, fgb, fgg, kng1
nfil3-5, nfil3-6
camk1gb, per2
opn1mw1, opn1sw2, tefa
Protein Polymerization
Melanosome Organization
fgb, fgg
gpr143, pmela, tyrp1b

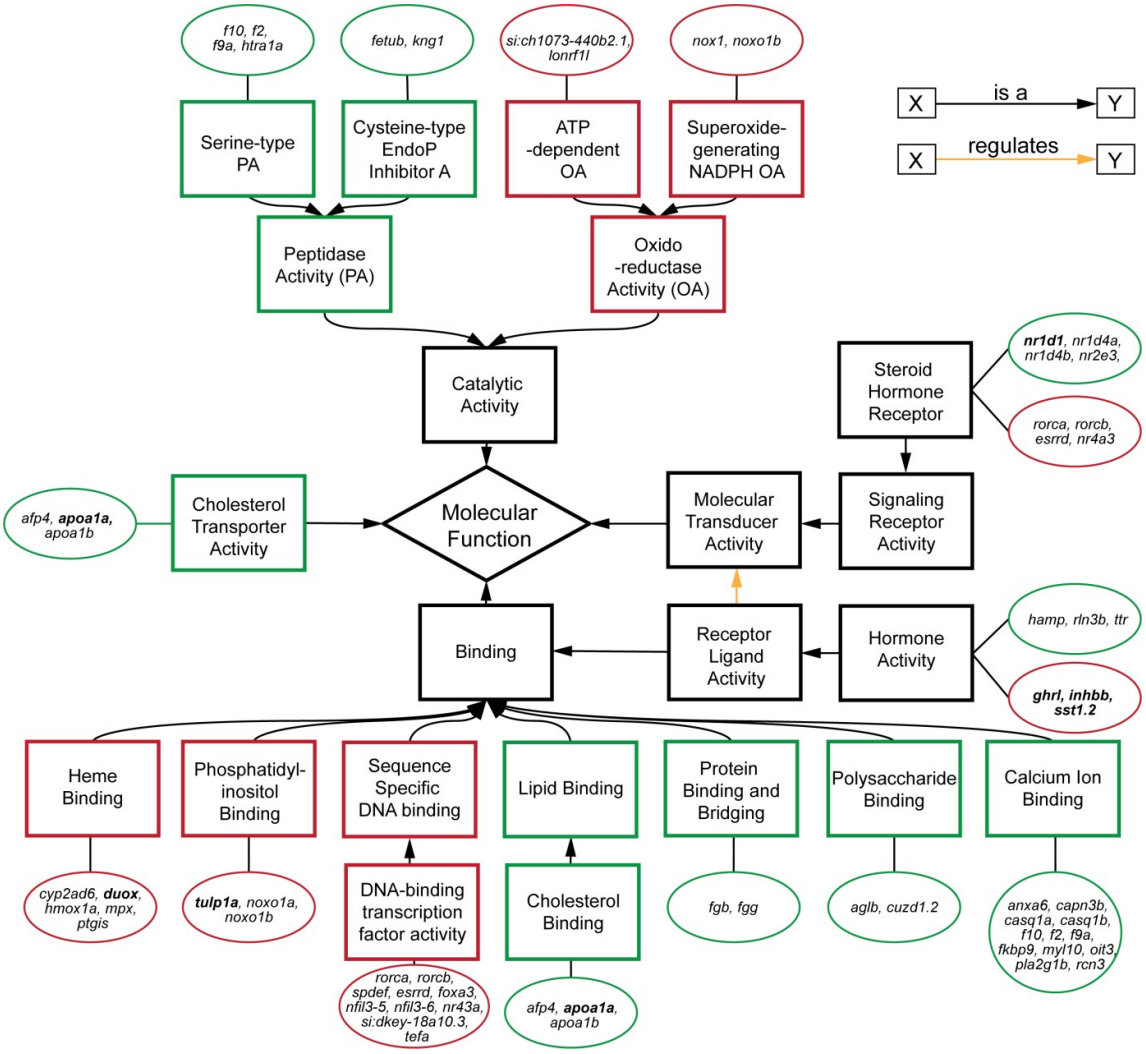

Figure 2. Subset of relevant, enriched GO terms (boxes) for biological processes (top) and molecular functions (bottom) of DEGs (circles) in the transcriptome. Genes tested by RT-PCR are in bold. Red outlines are down-regulated terms and genes, green outlines are up-regulated.

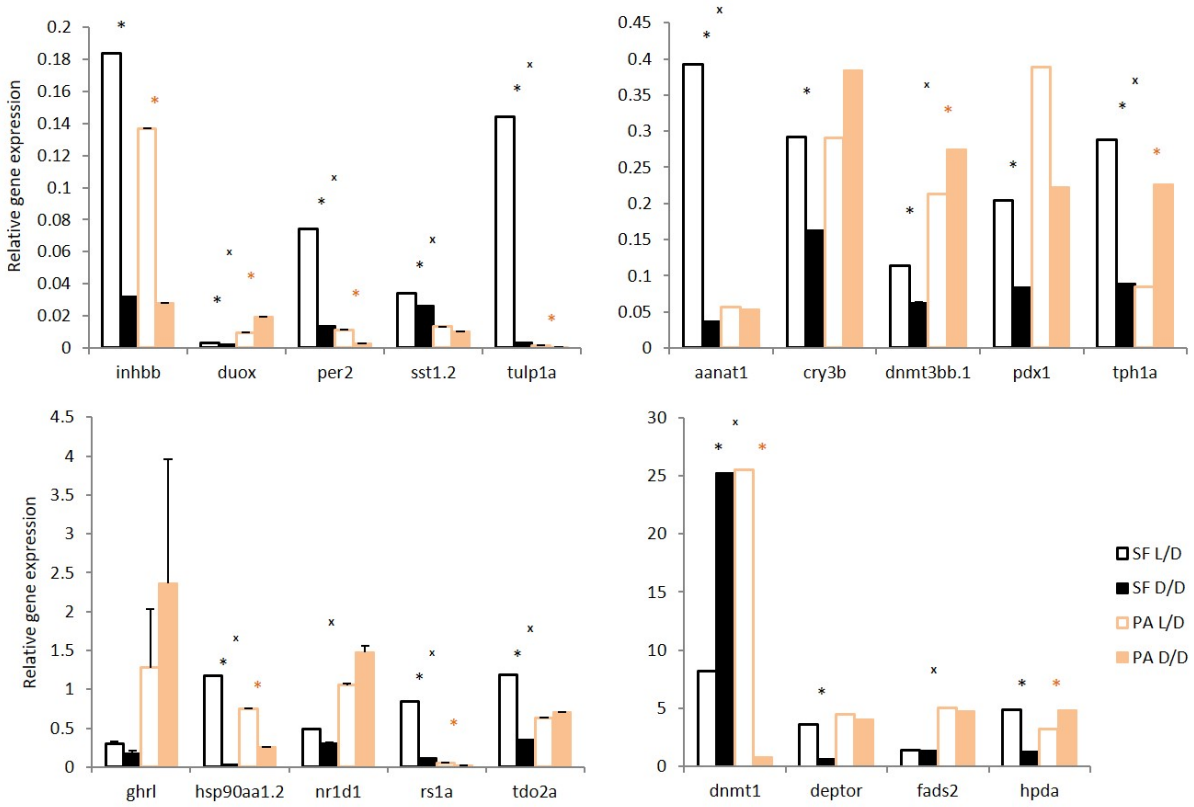

Figure 3. Normalized relative expression levels of genes in D/D and L/D SF and PA determined by RT-PCR. (Error bars: SD; ANOVA with Bonferroni adjustments $p<0.05$ * for SF D/D vs. SF L/D; * for PA D/D vs. PA L/D; ^{X} for SF vs. PA,).

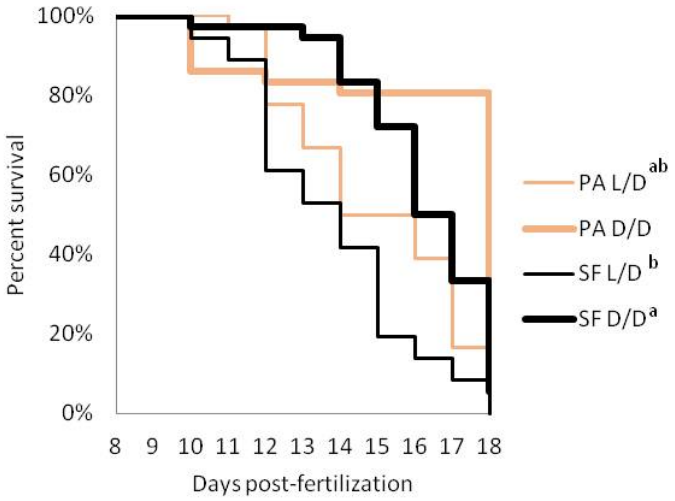

Figure 4. Survival curve of starvation resistance in *Astyanax mexicanus* surface fish (SF) and Pachón cavefish (PA) raised in complete darkness (D/D) or a normal photoperiod (L/D). Graphs show the percent of surviving fish (from the initial 36) on each day. Groups of SF and PA larvae from each condition were starved starting at 7 dpf. Vertical drops represent individuals lost at a given time point. Groups in the legend that share a superscript are not statistically different, p values calculated by Cox proportional hazards model followed by generalized linear hypothesis test.

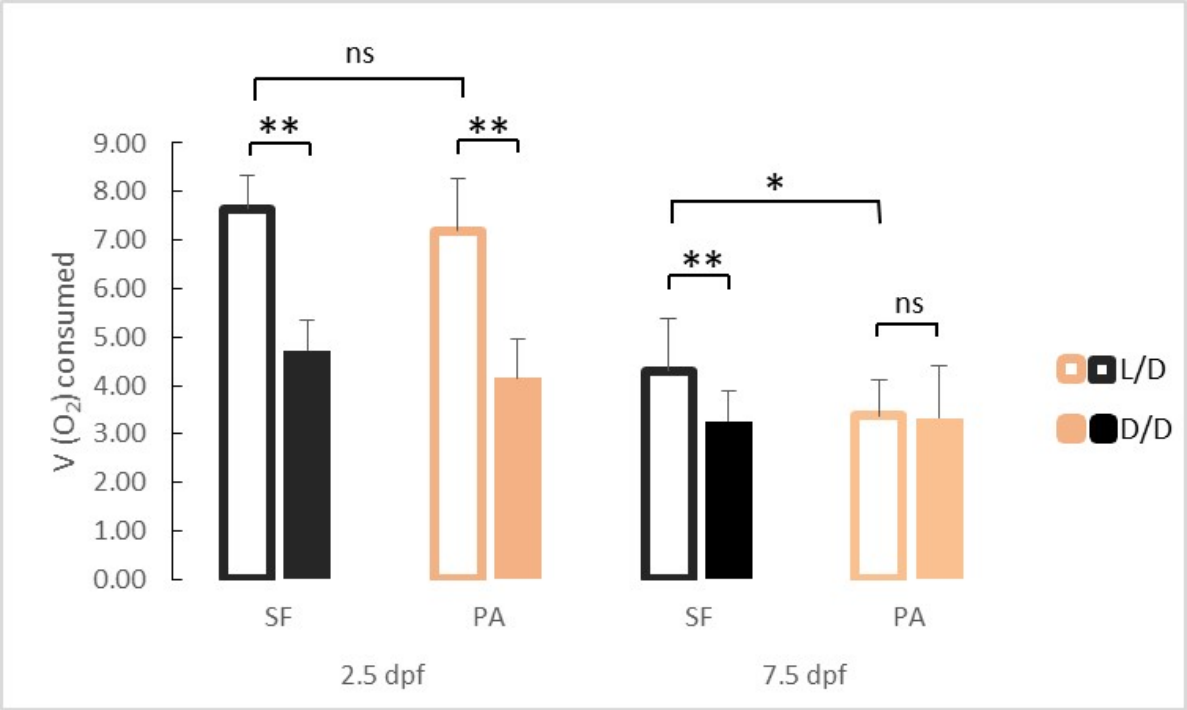

Figure 5. Average oxygen consumption at 2.5 and 7.5 dpf in SF and PA larvae kept in D/D versus L/D conditions (N = 18 - 25 larvae/group). (Error bars represent standard deviation, ns: not significant, *p<0.05, **p<0.01 as calculated by ANOVA and Tukey HSD Test.)

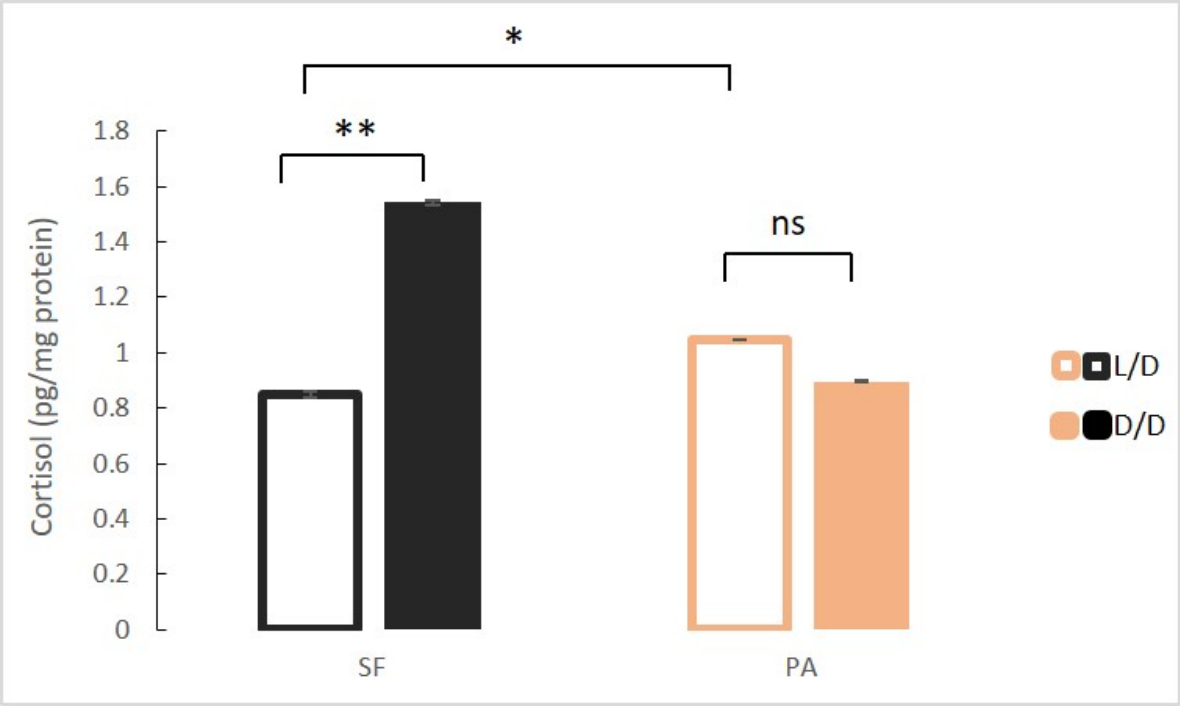

Figure 6. Mean cortisol levels in adult surface fish (SF) and Pachón cavefish (PA) kept in D/D or L/D conditions for 1.5 to 2 years (N=4/group). (Error bars represent SD in three technical replicates, ANOVA and Tukey HSD Test: Ns – not significant, *p<0.05, **p<0.01).

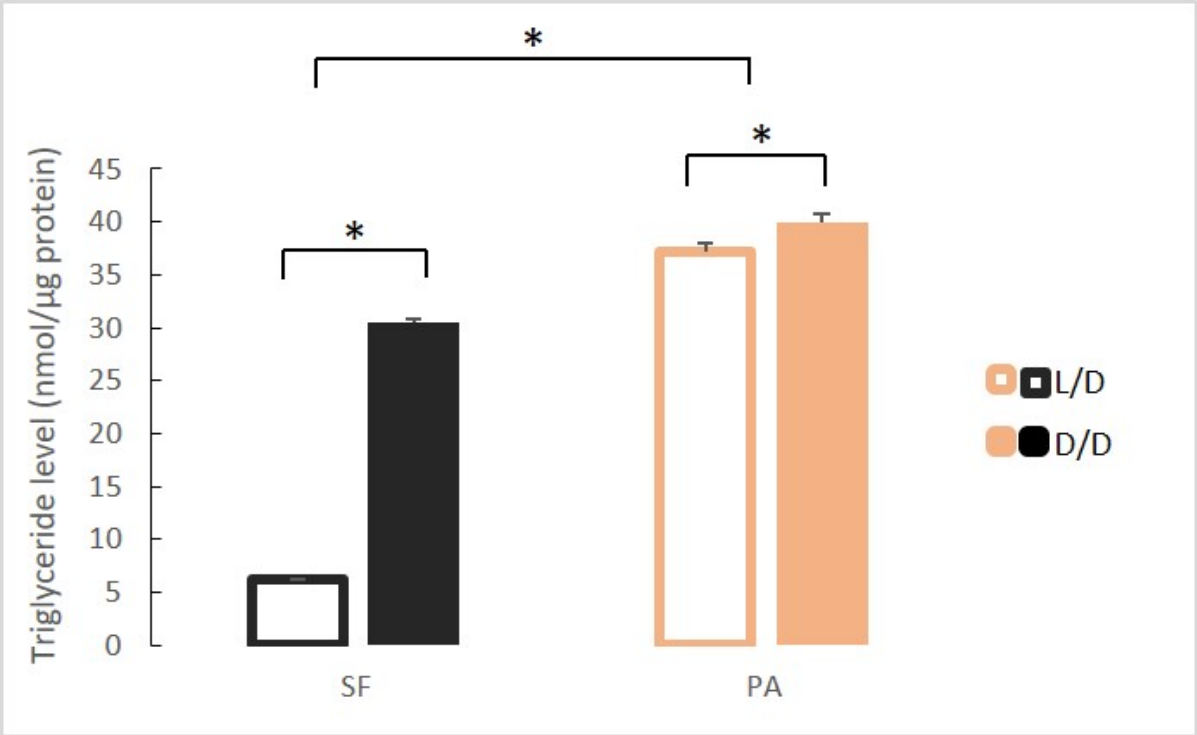

Figure 7. Mean triglyceride levels in SF and PA raised under D/D versus L/D conditions for approximately 1 year since < 24 hpf. (Error bars represent standard deviation. *p<0.01; ANOVA and Tukey HSD Test).

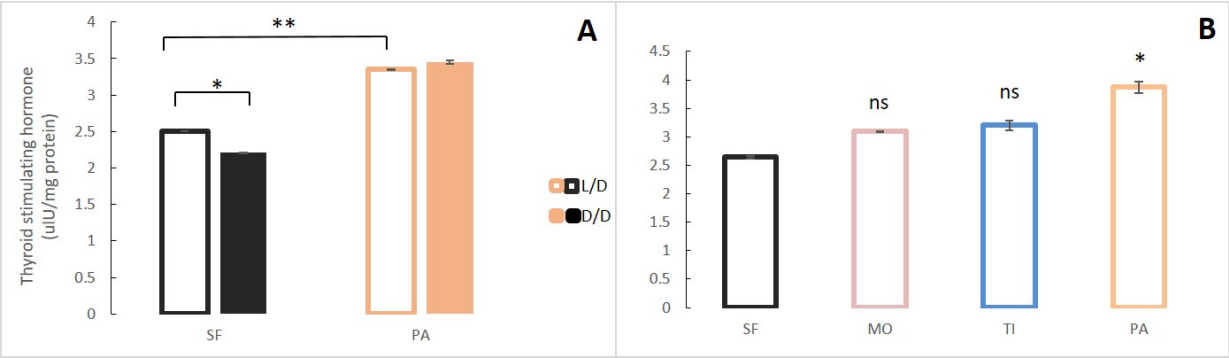

Figure 8. A. Mean Thyroid stimulating hormone (TSH) levels normalized by protein concentration in adult surface fish (SF) and Pachón cavefish (PA) kept in D/D or L/D conditions for 1.5 to 2 years. B. Mean TSH levels in SF and 3 different CF populations: Pachón (PA), Tinaja (TI) and Molino (MO) caves. (Error bars represent SD in three technical replicates. N ranges from 3-8 fish/group; * $p<0.05$; ** $p<0.01$ as calculated by ANOVA and Tukey HSD Test. In B. ns or * denotes significance in comparison to SF.)

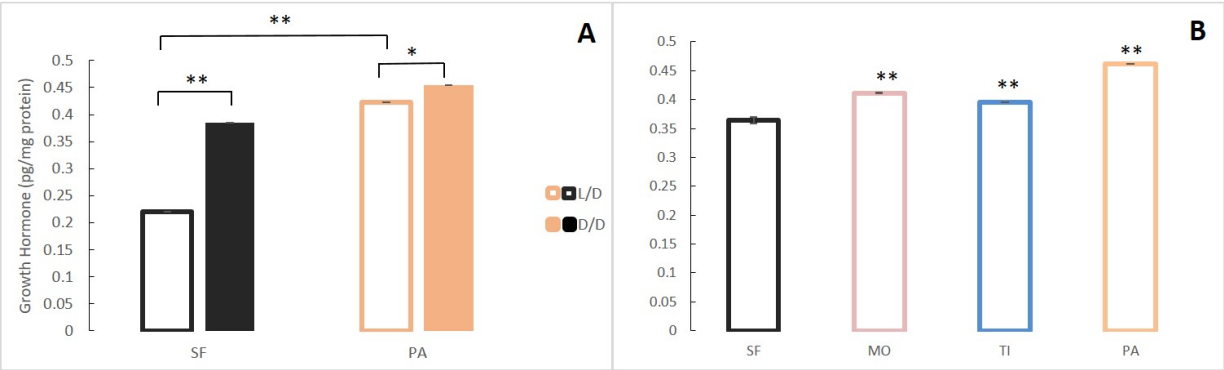

Figure 9. A. Mean growth hormone (GH) levels normalized by protein concentration in adult surface fish (SF) and Pachón (PA) cavefish kept in D/D or L/D conditions for 1.5 (SF) and 2 years (PA) since < 3 dpf. B. Mean GH levels in 3-4 month old SF and 3 different CF populations: PA, Tinaja (TI), and Molino (MO). (Error bars represent SD in three technical replicates. N = 3 to 8/group. *$p<0.05$; **$p<0.01$ as calculated by ANOVA and Tukey HSD Test. In B, **$p<0.01$ compared to SF).

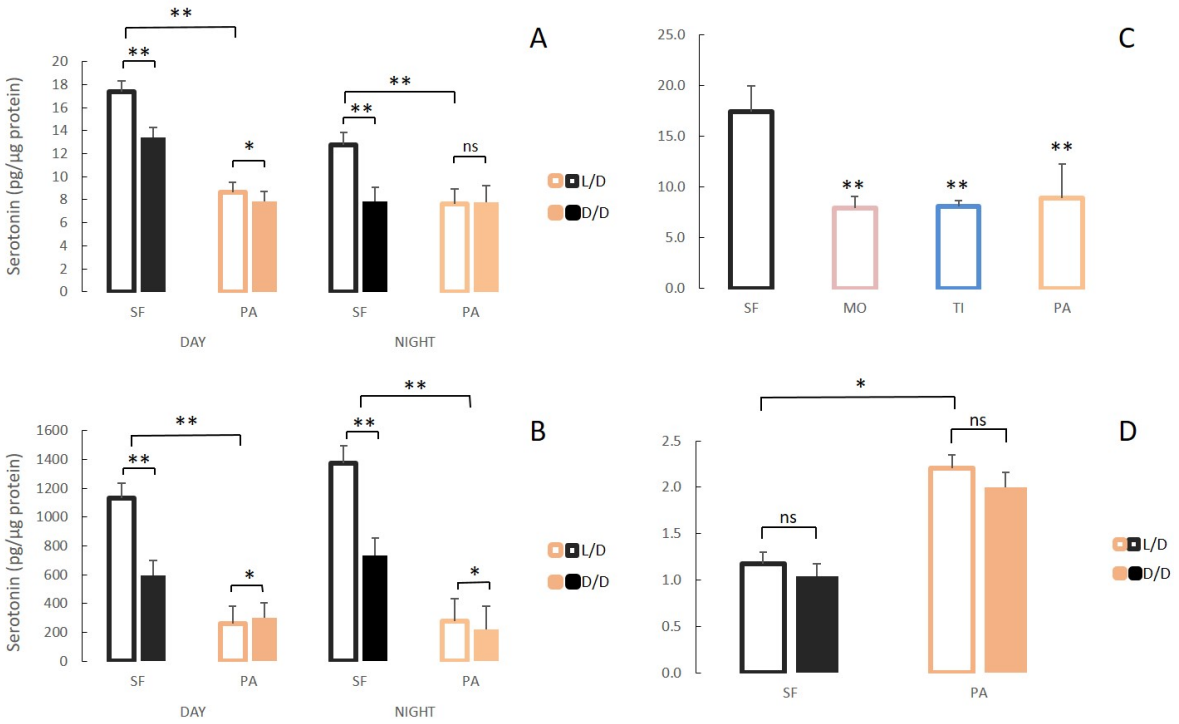

Figure 10. Serotonergic system changes in adults and larvae of light/dark (L/D)- and dark/dark (D/D)-reared surface fish and cavefish. A, B. Serotonin levels in adult brains (A) and bodies (B) of D/D and L/D reared surface fish (SF) and Pachón cavefish (PA) collected in the middle of the day (DAY) and the middle of the night (NIGHT). (Error bars represent the standard error of the means.) C. Mean serotonin levels in brains of adult SF and 3 different CF populations: Molino (MO), Tinaja (TI) and PA. D. Mean serotonin levels in pooled samples of 5 larvae aged 7 dpf placed in the experiment within first few hours post fertilization. (Error bars SEM; ns – not significant, *p<0.05; **p<0.01 as calculated by ANOVA and post-hoc Tukey HSD Test. In C, **p<0.01 vs SF. The number of each fish type subjected to analysis ranged from 4 to 10 per group.)

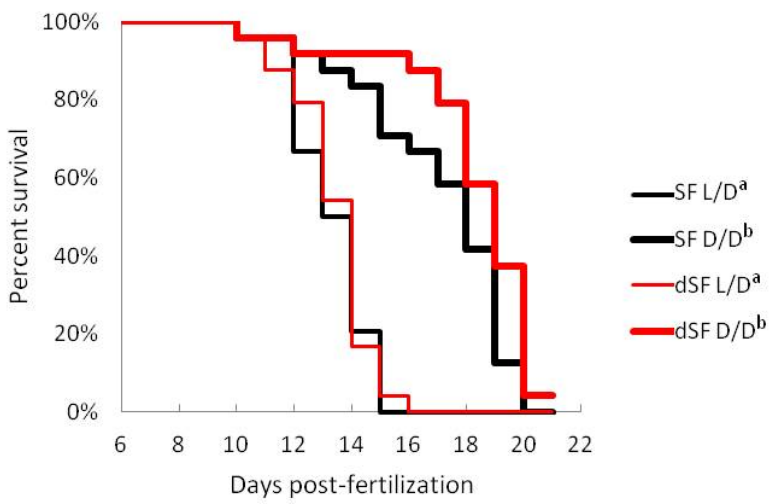

Figure 11. Survival curve of starvation resistance in F1 offspring of surface fish kept in normal light/dark photoperiod (SF) and surface fish raised in total darkness for 2 years (dSF). Graphs show the percent of surviving fish (from the initial 24) on each day. A. One group of larvae from each fish type (SF, dSF) and each lighting condition (D/D, L/D) was starved starting at 7 dpf (a vs. b $p<0.0001$). Vertical drops represent individuals lost at a given time point, groups in the legend that share a superscript are not statistically different, p values calculated by Cox proportional hazards model followed by generalized linear hypothesis test.

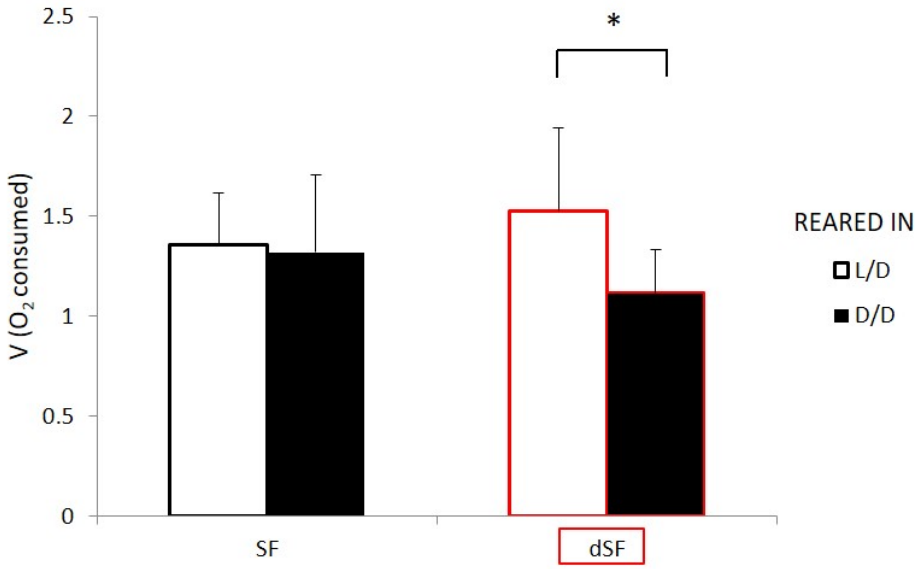

Figure 12. Average oxygen consumption of 11 dpf F1 offspring surface fish kept in the normal light/dark photoperiod (SF) and surface fish kept in total darkness for 2 years (dSF). Each group of offspring was exposed to D/D or L/D conditions within first 24 hpf. (Error bars represent standard deviation; *$p<0.05$, as calculated by ANOVA and Tukey HSD Test.).